Received: 1 February 2022 | Revised: 15 March 2022 | Accepted: 3 April 2022

DOI: 10.1002/nano.202100354

RESEARCH ARTICLE

Nano Select WILEY

Injectable and self-healing biobased composite hydrogels as future anticancer therapeutic biomaterials

Musammir Khan[1,2] | **Janne T. Koivisto**[1,3] | **Minna Kellomäki**[1]

[1]Biomaterials and Tissue Engineering Group, BioMediTech Institute, Faculty of Medicine and Health Technology, Tampere University, Tampere, Finland

[2]Department of Chemistry, University of Wah, Quaid Avenue, Wah Cantt, Rawalpindi, Punjab 47040, Pakistan

[3]Department of Laboratory Medicine, Karolinska Institute, Huddinge, Stockholm, Sweden

Correspondence
Minna Kellomaki, Biomaterials and Tissue Engineering Group, BioMediTech Institute, Faculty of Medicine and Health Technology, Tampere University, Korkeakoulunkatu 10, 33720 Tampere, Finland.
Email: minna.kellomaki@tuni.fi

Abstract

Self-healing composite hydrogels are prepared from sustainable biopolymers by a green chemistry approach and analyzed by physicochemical and mechanical characterization techniques for future injectable anticancer biomaterials. Water-soluble chitosan (WSC) was prepared by grafting polyethylene glycol (PEG), glutamic acid and gallic acid onto the chitosan chain by carbodiimide chemistry. This WSC showed fast gelation ($t \approx < 60$ seconds) with benzaldehyde-terminated 4-arm-PEG as a crosslinker through an amine/aldehyde Schiff base reaction. The compression modulus of these gels can be controlled between 6 and 67 kPa, which was dependent on both the crosslinker content as well as the total solid content (T%). It showed injectability and complete self-healing ability at the lower solid content (T = 2%). The hydrogel nanocomposites (HNCs) were synthesized together with gold (Au) and silver (Ag) nanoparticles (NPs) and tested for cytotoxicity using fibroblast cells (WI-38) for 48 hours, which showed good biocompatibility. The in-vitro assay against cancer cells (U87MG) for 48 hours indicated that only the HNCs with incorporated AuNPs were effective agents for cancer cell apoptosis in contrast to pristine gel, pure NPs (Ag and AuNPs) and HCNs with AgNPs. Therefore, these HNCs could be effective chemotherapeutic materials for designing anticancer nanomedicines in the future.

KEYWORDS

anticancer assays, biocompatibility, biopolymers, composites hydrogels, injectable/self-healing

1 | INTRODUCTION

Composite hydrogels with self-healing ability made up of natural and synthetic polymers with tunable mechanical and tissue mimicking capability are presenting an emerging class of biomaterial with superior characteristics than the parent materials.[1] Nanocomposites (NCs) made up of composite hydrogels with incorporated metallic nanoparticles (MNPs) have several intriguing properties, such as antimicrobial, anticancer and responsiveness to electric or magnetic field stimuli. These MNPs might be gold (Au), silver (Ag), nickel (Ni) or metal oxides of iron (Fe_2O_3), titania (TiO_2) and zirconia (ZrO_2).[2]

The incorporation of NPs into natural-based biomaterials works as an activated therapeutic by enhancing the cellular interactions in wound repair and scaffolding performance.[3] Previously, the wound healing ability and antibacterial characteristics had been

combined in a single composite material of AgNPs/chitosan.[4]

Chitosan is a polysaccharide with excellent biological properties, such as antibacterial, wound-healing ability, biodegradability and immunological activity, and hence many of its derivatives are potent candidates for gene delivery, cell culture and tissue engineering areas.[5] However, pure chitosan with about 85% degree of deacetylation (DD) is insoluble at physiological pH, so it can be modified into several versions of water-soluble chitosan (WSC) such as grafting of polyethylene glycol (PEG (FDA approved)),[6] carboxymethyl modified,[7,8] arginine,[9] dopamine/catechol group,[10] and gallic acid (GA) grafted-chitosan.[11] Among synthetic hydrophilic and biocompatible polymer crosslinkers, the multi-arm-PEG functionalized with aldehyde groups is very attractive owing to its high flexibility, biodegradable ester linkages and antifouling ability.[12,13]

GA (3,4,5-trihydroxybenzoic acid) is a putative compound in tannin and is the main polyphenolic compound in grapes, berries, mango, areca nut, walnut, green tea. It has remarkable biological activities, such as higher antitumor sensitivity than normal cells, anti-carcinogenic and anti-viral, antibacterial, antifungal, anti-inflammatory and anti-malarial properties. This compound has also been described for its excellent free radical or antioxidant activities.[14,15] The antioxidant-biopolymer conjugates, in this case GA-chitosan, exhibit amplified bioactivities, such antioxidant, antibacterial, anticancer and inhibitory effects on digestive enzymes when compared to the free GA or biopolymer. This conjugation can be performed by either enzyme or chemical modification.[16]

Green chemistry has revolutionized the field of material science and nanotechnology to design low-cost, biocompatible, and biodegradable materials with desired mechanical properties and minimum side product formation.[17] The use of GA as green capping and reducing agents for the synthesis of Ag and Au NPs is an attractive strategy,[18] thus avoiding the use of toxic reductants such as hydrazine and sodium borohydride.[19]

The soft-gel nanocomposites can be obtained by host–guest interactions in which gel matrix (chitosan) acts as a "host" and MNPs (AuNPs, AgNPs) with appropriate capping agent (GA) is working as "guest" through van der Waals interactions and hydrogel bonding.[20] Moreover, the presence of amine groups in the WSC biopolymer and aldehyde groups in the benzaldehyde-functionalized star-PEG (PEG-BA) crosslinker would result in self-healing 3D hydrogels by reversible Schiff-base linkages, thus mimicking a bioinspired natural self-recovery mechanism.[21,22]

AuNPs bioconjugates can rapidly convert strongly absorbed light into localized heat and thus can also work as selective photothermal cancer agents without affecting healthy cells.[23] The presence of mobile negatively charged citrate/GA functionality on these NP surfaces provides an exchange opportunity for positively charged moieties, thus enhancing cell uptake for designing anticancer pharmaceuticals.[24] In addition to physicochemical properties, this surface charge has a substantial effect on the enhanced permeability and retention (EPR) effect, which contributes to nanocarriers (diameter <100 nm) drug penetration and accumulation into cancer cells through passive targeting and endocytosis.[25] The current modalities of cancer, such as chemo- or radiation therapy, have undesirable consequences of nonspecific dissemination, high dose requirements and poor bioavailability. Hence, the chitosan-based nanocomplexes have evade these issues, ameliorating the dispatch of therapeutic agents to tumor cells via a targeted approach.[26,27]

Here in this work, a self-healing composite hydrogel was prepared from chitosan biopolymer, WSC, using benzaldehyde-terminated star-branched PEG as a crosslinker. The gel components and their composition were analyzed by various physicochemical characterization techniques. The gel was comprehensively investigated by mechanical characterization in order to get an optimized composition for injectable application. The gel nanocomposites with MNPs of Ag and Au were applied for in-vitro applications against fibroblast cells (WI-38) and cancer cells (U97 MG) for 48 hours.

2 | EXPERIMENTAL SECTION

2.1 | Materials

All the chemicals were purchased from Sigma Aldrich, that is, $AgNO_3$ (99%), $HAuCl_4$ (99%), trisodium citrate dihydrate ($Na_3Ct.2H_2O$) (99%), GA (99%), Chitosan (M_w = 50–190 kDa, DD = ~80 %), L-glutamic acid (≥99%), N-(3-dimethylaminopropyl)-N′-ethylcarbodiimide hydrochloride (EDC) (≥99%), and 4-formyl benzoic acid (97%). The 4-arm polyethylene glycol (4-arm PEG) (95% M_w = 10 kDa) and PEG-5k 95% was purchased from JenKem Technology USA.

2.2 | Methods

2.2.1 | Preparation of silver and gold nanoparticles

For this study we used GA-capped MNPs of Ag and Au obtained under optimum conditions, as reported in our recent work,[18] that is, AgNPs (size = 50 nm, zeta potential = -34 mV and AuNPs (size = 32 nm, zeta potential = -36

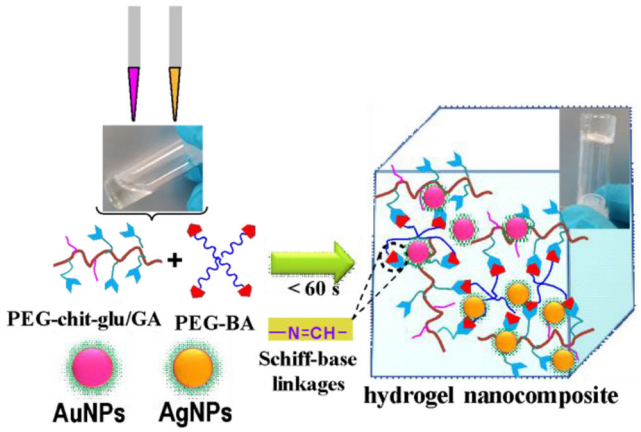

SCHEME 1 Preparation of 3D composite hydrogel from WSC (chit-glu-PEG/GA), PEG-BA crosslinker and metallic NPs (AgNPs & AuNPs)

mV). The concentration/number density of these NPs was determined using UV/visible absorbance data according to the previously established quantification protocol for both kinds of NPs.[28]

2.2.2 | Preparation of WSC and star-PEG crosslinker

Both the components of the gel, WSC (chit-glu-PEG/GA) and star-PEG crosslinker, were prepared by the same carbodiimide chemistry approach,[29] except with the addition of two other reagents, PEG (5 k) and GA and henceforth will be represented by the symbol WSC (chit-glu-PEG/GA), throughout the text.

2.2.3 | Preparation of 3D composite hydrogel

The composite hydrogel was prepared using different amounts of WSC and benzaldehyde-terminated 4-arm PEG (PEG-BA) crosslinker (Scheme 1).[29] Both the WSC biopolymer and PEG-BA crosslinker were separately dissolved in deionized (DI) water in a glass vial to obtain a homogeneous solution. For each desired composition, the specific amount of PEG-BA crosslinker solution was added into the WSC matrix using micropipette and then vortexed for 15 seconds, which resulted in quick gelation of the hydrogel within 60 seconds.

Note, for biocompatibility and anticancer activity assays, the composite hydrogels were incorporated with ex situ prepared different number density (NPs per mL) of AgNPs and AuNPs (5 μL, 10 μL, 20 μL) stock solutions (~ 1×10^9 NPs, 2×10^9 NPs, 3×10^9 NPs).

2.3 | Characterization techniques

For proton nuclear magnetic resonance spectroscopy (^{1}H NMR) analysis, chit-glu was dissolved in D_2O (10 mg mL^{-1}) and pure chitosan (10 mg mL^{-1}) in 1.5% D_2O solution of CD_3COOD. PEG and PEG-BA were dissolved in $CDCl_3$ (15 mg mL^{-1}). The NMR spectra were recorded on a Varian Mercury 300 MHz spectrometer using tetramethylsilane (TMS) as the internal standard.

Fourier transform infrared spectroscopy (FTIR) measurements were made with a Bruker optics tensor 27 using attenuated total reflectance (ATR) mode, between 650 and 3500 cm^{-1}, using 16 scans and a resolution of 4 cm^{-1}.

Differential scanning calorimetry (DSC) analyses were carried out on a NETZSCH DSC 204F1 Phoenix instrument with an automatic sampler changer. The sample was taken and pre-weighed in a 100 μL Al pan with pierced lid and heated twice under an inert gas (N_2) atmosphere from 25 to 220°C with a heating rate of 10°C min^{-1} and cooled down at a rate of 40°C min^{-1} between heating. In the final cycle, the sample was heated from 25 to 350°C.

For mechanical characterization of hydrogels, hydrogel discs of different composition samples (volume 500 μL, cross-section diameter (D) = 8.0 ± 1 mm and height (H) = 7.0 ± 1 mm) were prepared in a plastic syringe and covered with paraffin film. The D and H of the samples were measured with a digital Vernier caliper. Compression testing was done with a Bose BioDynamic ElectroForce Instrument 5100 using WinTest 4.1 software (TA Instruments, USA). The number of parallel compression samples (n) was more than three ($n > 3$) and the results were averaged ± SD. The testing was carried out under uniaxial, unconfined compression in air at ambient pressure and temperature. The compression was carried out with a speed of 10 mm min^{-1} and up to 65% of the original sample height. From the results, the stress (kPa) value was calculated as a force per unit area and the strain (mm mm^{-1}) as a displacement per unit height. The slope of the linear region of the stress versus strain curve (i.e., 15–35% strain), yields the compression modulus.

2.4 | In vitro cell viability assay

The human lung fibroblast cell line WI-38 (from ECACC, Public Health England, UK) was cultured with Dulbecco's Modified Eagle Medium/Ham's Nutrient Mixture F-12 (DMEM/F-12 1:1; Thermo Fisher Scientific) supplemented with 10% fetal bovine serum (South American origin, Biosera, Finland) and 0.5% Penicillin/Streptomycin 100 U mL^{-1} (P/S; Thermo Fisher Scientific). During biocompatibility testing the cells were trypsinized, counted and plated on top of the hydrogel at density 20,000–30,000 cells cm^{-2}

for three days. For viability analysis, the cultures were stained using a LIVE/DEAD cell viability/cytotoxicity assay kit (Molecular probes, Thermo Fisher Scientific). In the staining assay Calcein-AM (0.2 μM, $\lambda^{excitation} = 488$ nm) stains live, intact cells green and Ethydium homodimer-1 (0.8 μM, $\lambda^{excitation} = 568$ nm) stains dead cells red. After 30 minutes incubation, the cells were imaged with an Olympus IX51 inverted fluorescent microscope and an Olympus DP30BW digital camera (Olympus, Finland).

2.5 | In vitro anticancer activity against U87MG cells

The U87MG cells were donated by research a group from Solna, Sweden (Karolinska Institute). The cells were grown on Dulbecco's modified Eagle's medium (DMEM) (Hyclone, Logan, UT) supplemented with 10% fetal bovine serum (FBS) and cultured at 37°C in humidified atmosphere of 5% CO_2 environment.[30] The cells were plated at a density of 20,000–30,000 cells cm^{-2} on top of the hydrogel, while replacing the media after each 3 days. The cultures were stained using a LIVE/DEAD cell viability/cytotoxicity assay kit (Molecular probes, Thermo Fisher Scientific). In the staining assay Calcein-AM (0.2 μM, $\lambda^{excitation} = 488$ nm) stains live, intact cells green and Ethydium homodimer-1 (0.8 μM, $\lambda^{excitation} = 568$ nm) stains dead cells red. After 30 minutes incubation, the cells were imaged with an Olympus IX51 inverted fluorescence microscope and an Olympus DP30BW digital camera (Olympus, Finland).

3 | RESULTS AND DISCUSSION

The composite hydrogel was prepared from WSC, (chit-glu-PEG/GA) and benzaldehyde-terminated 4-arm PEG (PEG-BA) (Scheme 1) according to our previous protocol with slight modification.[31] The hydrogel nanocomposites (HNCs) with MNPs were prepared by the addition of AuNPs and AgNPs together with gel components, which resulted in quick gelation in <60 seconds.

The PEG raw polymer and its derivatives were characterized by FTIR spectroscopy (Figure 1). The characteristic peak for the carboxyl group –COOH is observed at 1734 cm^{-1} in the case of PEG-COOH (Figure 1A), while for the aldehyde group (-CHO) a band appeared at 1708 cm^{-1}, confirming the successful formation of PEG-BA. Chitosan modified with PEG showed the characteristic PEG C-H stretch at 2875 cm^{-1} (Figure 1B (ii)). The characteristic band of PEG oxygen C-O-C bending vibration at 1095 cm^{-1} also appeared in the modified chitosan (chit-glu-PEG) and shifted towards 1102 cm^{-1}, which indicated the successful conjugation and H-bonding with the chitosan cationic amine groups.[32] The amide (II) of glutamic acid merged and weakly appeared at 1528 cm^{-1} in case of all the derivatives and the gel samples (Figure 1B (ii-v)). Similarly the –C = O symmetric stretching appeared at 1406 cm^{-1}.[33] The asymmetric $-CH_2-$ stretching for PEG merged with glutamic acid and appeared at 1466 cm^{-1}.[34]

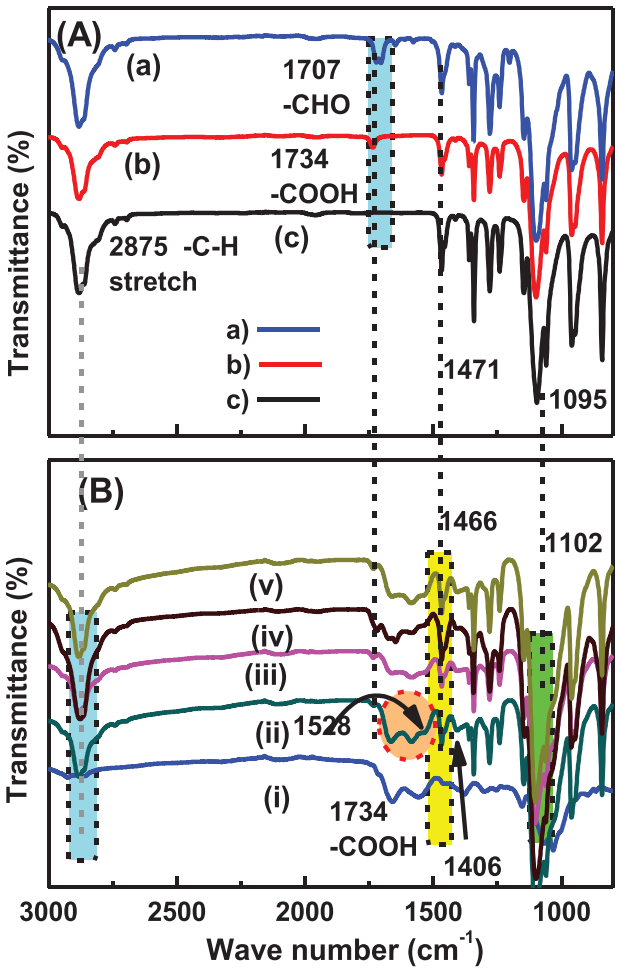

FIGURE 1 FTIR spectra of (A) (a) 4-arm-PEG (10 k), (b) PEG-COOH, (c) 4-arm-PEG-BA, (B) (i) pure chitosan, (ii) chit-glu-PEG, (iii) chit-glu-PEG/GA, (iv) chit-glu-PEG (gel-A) and (v) chit-glu-PEG/GA (gel-B)

The ^{1}H-NMR characterization of the raw PEG-OH, 4-arm PEG and their derivatives (Figure 2), shows the characteristic NMR signals of the different functional groups. The –CH2-COOH characteristic NMR peak of PEG-COOH (Figure 2A) at 2.6 ppm is indicated.[35] While in case of modified chitosan, WSC the characteristic ^{1}H-NMR resonance for glutamic acid appeared at 2.8 ppm (2H) indicating successful grafting.[16]

The grafting of GA onto the chitosan chain was further confirmed from the characteristic UV-visible SPR peak (Figure 3). Pure GA showed an SPR peak (red line) at 263 nm, while the chitosan derivative (chit-glu-PEG) (black

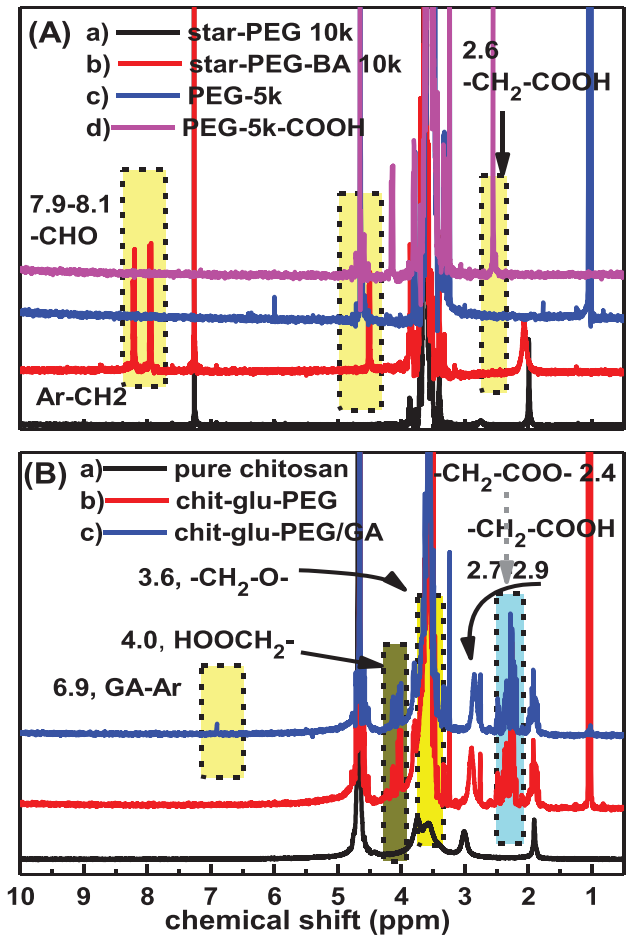

FIGURE 2 H-NMR spectra of the (A) a) star-PEG (10 k), b) EG-BA, c) pure PEG (5k), d) PEG-COOH (5k), and (B) a) chitosan, b) chit-glu-PEG and c) chit-glu-PEG/GA

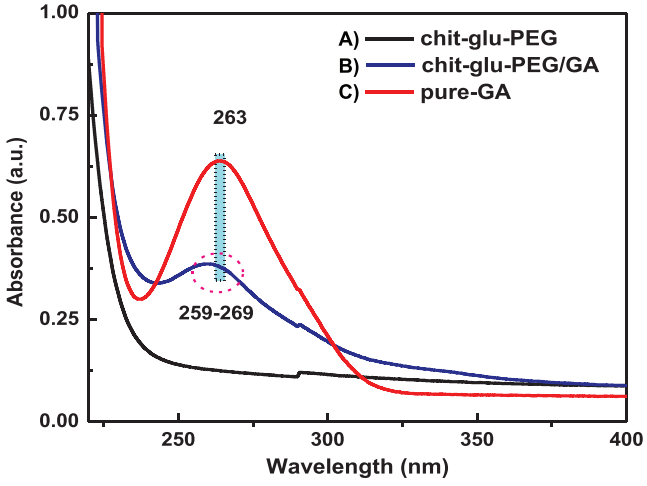

FIGURE 3 UV-visible spectra of A) PEGylated chitosan (chit-glu-PEG), B) chit-glu-PEG/GA), C) pure gallic acid (GA)

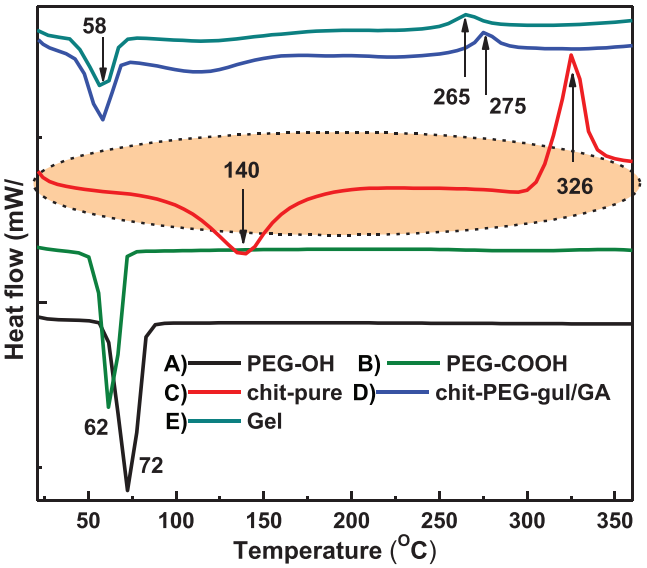

FIGURE 4 DSC spectrum of the pure PEG and chitosan biopolymer at various stages of modification. A) pure PEG-OH, B) PEG-COOH, C) pure chitosan, D) chit-glu-PEG/GA, E) gel

line) did not show any peak. The same derivative conjugated with GA (chit-glu-PEG/GA) showed the characteristic SPR peak for GA in the range 259–269, with a slight red shift indicating a low energy n-π^* and π-π^* transition, confirming the successful conjugation of GA onto the chitosan chain.[36,37]

The DSC spectrum of PEG-OH, PEG-COOH (Figure 4) shows only a single melting temperature at 72°C for raw PEG-OH and drops after modification for PEG-COOH to 62°C. Similarly, the chitosan derivatives during different stages of modification showed that the melting and decomposition temperatures of pure chitosan were 140 and 326°C, respectively. After successive modification the T_m and T_d dropped to 58 and 375/365°C, respectively.

The mechanical properties of the hydrogels were investigated by compression testing assay as a function of chit-glu-PEG/GA/PEG-BA (WSC/PEG-BA) ratios at constant total solid content (T = 6%) (Figure 5A) and as a function of T (%), while keeping constant polym/cross ratio (1:1) (Figure 5B). Note that the amount mentioned here of both the biopolymer (WSC) and the crosslinker (PEG-BA) is taken as weight (W/W) ratio and same is case with the T (%) in the final solution. The mechanical strength (compression modulus) was highest at (WSC/PEG-BA) ratio of 1:1 and increased when T (%) was increased. The (WSC/PEG-BA) ratio of 1:1 was taken as optimum and investigated further to find the injectable concentration (T%), which was ~ T = 2% (Figure 5A), with a compression modulus value of 6 ± 2 kPa. Note that as the crosslinker ratio was reduced ((WSC/PEG-BA) = 2:1) (A) or reducing the T% (3% and 2%) (B), in both cases, the fracture strength

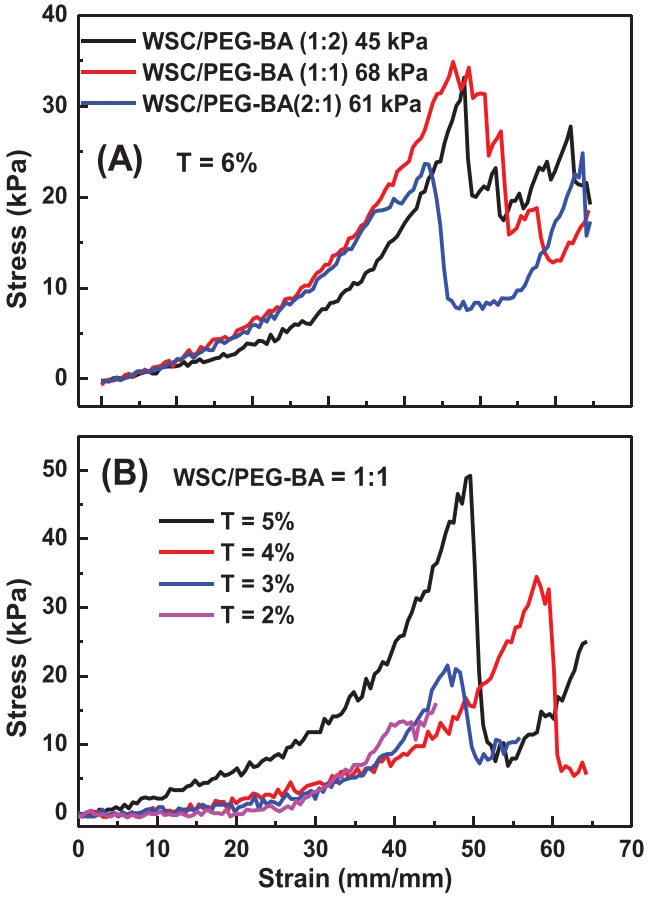

FIGURE 5 Compression testing of the prepared hydrogel samples A) at fixed T% (6%) and various (WSC/PEG-BA) ratios, B) at fixed (WSC/PEG-BA) ratios (1:1) and different total solid content (5%, 4%, 3%, 2%)

TABLE 1 Mechanical properties of the hydrogel as a function of crosslinker and total solid content

S. No.	(WSC/PEG-BA) [W/W]	Total solid content [T %]	Modulus [kPa]
1	1:2	6	45 ± 4
2	1:1	6	68 ± 5
3	2:1	6	61 ± 5
4	1:1	5	63 ± 5
5	1:1	4	25 ± 3
6	1:1	3	21 ± 3
7	1:1	2	6 ± 2

(ultimate strength that the material can endure without breaking) decreases and commences at 45% strain.

The mechanical properties of the hydrogels are summarized in Table 1 as a function of varying crosslinker content and total solid content, while keeping other parameters constant.

The mechanical properties of the hydrogels as a function of total solid content and (WSC/PEG-BA) ratios (Figure 6)

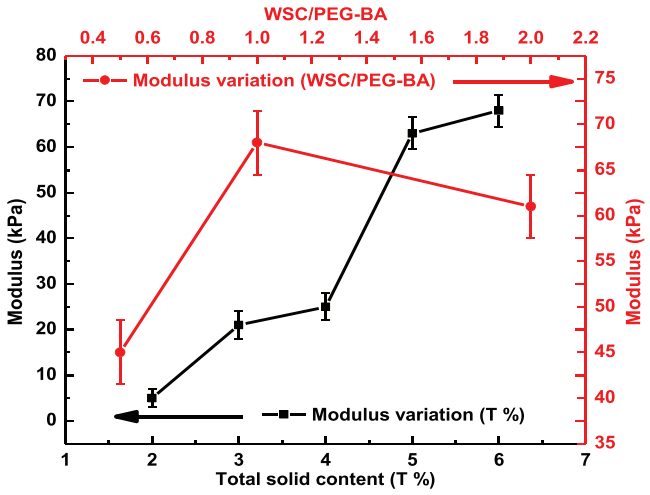

FIGURE 6 Compressive modulus of the hydrogels as a function of total solid content (T%) (left-bottom axis) and as a function of (WSC/PEG-BA) ratios (top-right axis)

indicated that deviating the (WSC/PEG-BA) ratios from 1:1 (modulus = 68 ± 5 kPa) (T = 6%) on both extremes shows a decrease in modulus values such as using ratios of 1:2 (modulus = 45 ± 4 kPa) and 2:1 (modulus = 61 ± 5 kPa). This indicates that there is no linear correlation between the polym/cross ratios and modulus values, but for an equal number of complementary groups (aldehyde and amine) available in the vicinity or (1:1) ratios, then there is more chance for molecular network formation rather than just merely rising crosslinker ratio.

This optimum ratio (1:1) was further investigated to check the mechanical factor at various T%, which showed a regular fall in the modulus values (Figure 6 bottom-left axis) as the T% was reduced. This shows that the spacing between the polymer network increases with high water contents, which makes the network a more mobile/flexible network with an obviously lower mechanical strength when moving from T = 6% to 2%.

3.1 | Injectability/self-healing experiment

The composite gel with (T = 2%, (WSC/PEG-BA) = 1:1) was investigated for injectability and self-healing ability in phosphate buffer saline (PBS, pH = 7.4) under ambient conditions (Scheme 2). The as prepared gel discs (original transparent) and colored red (A) were taken into 5 mL syringes (B) and then was injected through 22-gauge needle successively (C). The injected gels were kept in PBS (pH = 7.4) for 2 hours under ambient conditions (D). The self-healed gel was taken out of the syringes and were lifted with tweezers (F), showing it was free-standing under

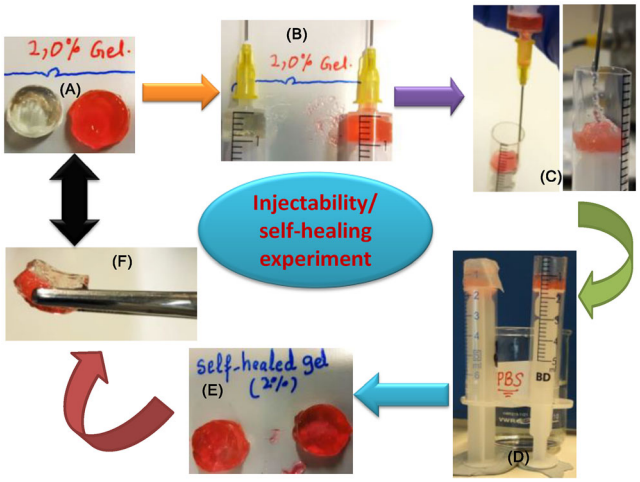

SCHEME 2 Injectability and self-healing experiment (WSC/PEG-BA = 1:1, T = 2%) gel: A) as prepared hydrogel discs, B) gels were taken into the syringes, C) gels were injected successively (red one followed by original transparent gel) through 18 gauge needle, D) injected gel as kept for 1 hours in PBS, E) self-healed gel, F) self-healed gel was lifted with tweezers, which proved its mechanical stability

stress and thus showing its fully recovered network structure (F = A).

3.2 | Gelation time

The rate of gelation, which is a mechanism of transforming the clear polymer solution into a well-shaped, self-standing elastic hydrogel, was investigated under ambient conditions by varying the total solid content (T%) in the gel. The gelation time (seconds) was inversely related to T%, as the T% was lowered from 6% to 2%, the gelation time was increased from 18 ± 4 seconds to 180 ± 6 seconds (Figure 7). This was because the overall gradually higher concentration (W) of the two components (WSC and PEG-BA) per total solvent amount (high T%), would lead to effective crosslink point formation due to the presence of reactive groups (amine and aldehyde) in the vicinity.

3.3 | In vitro biocompatibility assay

The biocompatibility of newly designed biomaterials by in vitro assays using target primary cells or cell lines is a prerequisite for materials used for clinical applications.[38] However, the in vivo complexity could not be captured here, but it is providing an indispensable part of evaluation of biomaterials for medical implants and drug delivery uses.[39] The in vitro cytocompatibility of these hydrogels (T = 4%, modulus = 25 ± 3 kPa) was tested using fibroblast

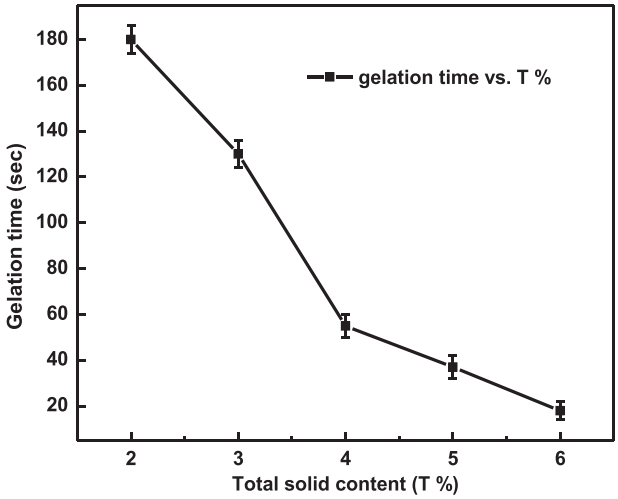

FIGURE 7 Gelation time (seconds) as a function of total solid contents (T%) in the composite gel

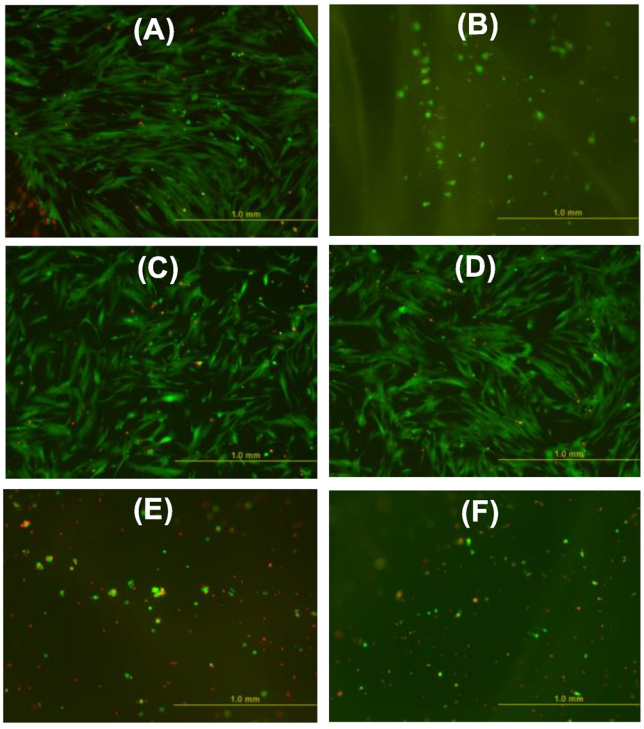

FIGURE 8 WI-38 cells cultured for 48 hours; A) blank, B) chit-glu-GA/PEG gel only, C) AgNPs, D) AuNPs, E) chit-glu-GA/PEG-AgNPs, F) chit-glu-GA/PEG-AuNPs. Scale bar is 1 mm

cells (WI-38) for 48 hours (Figure 8). The results indicate that all the blank hydrogels, pure NPs and HNCs were biocompatible toward these healthy cells. For the nanocomposites, different amounts (numbers) of NPs were added to the gel components. Note that due to almost similar effects on the physicochemical, mechanical and in vitro assays, only representative pictures of NPs (~1×10^{-9} NPs per well)

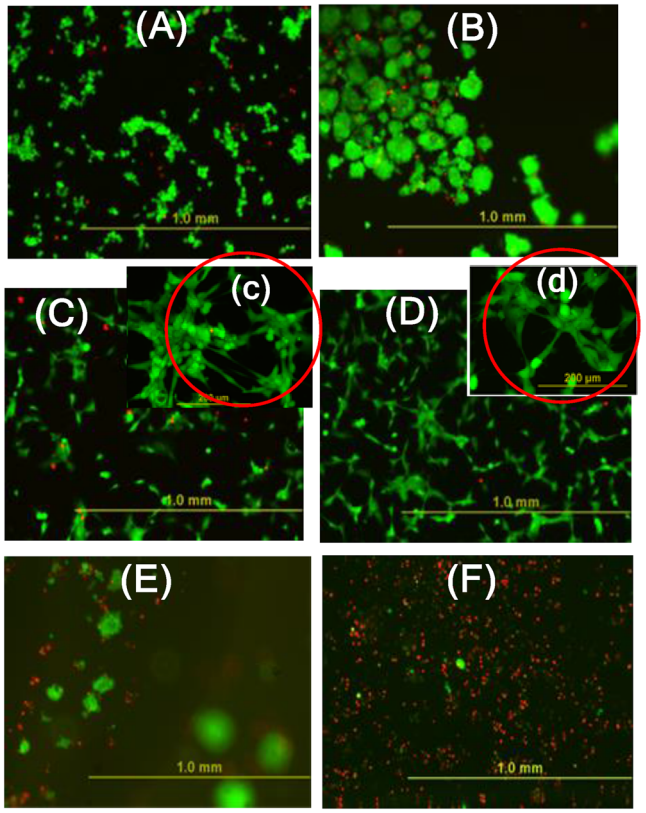

FIGURE 9 In vitro anti-cancer activity against U87 MG cells: A) blank, B) chit-glu-GA/PEG gel only, C) AgNPs, D) AuNPs, E) chit-glu-GA/PEG-AgNPs, F) chit-glu-GA/PEG-AuNPs. Scale bar is 1 mm

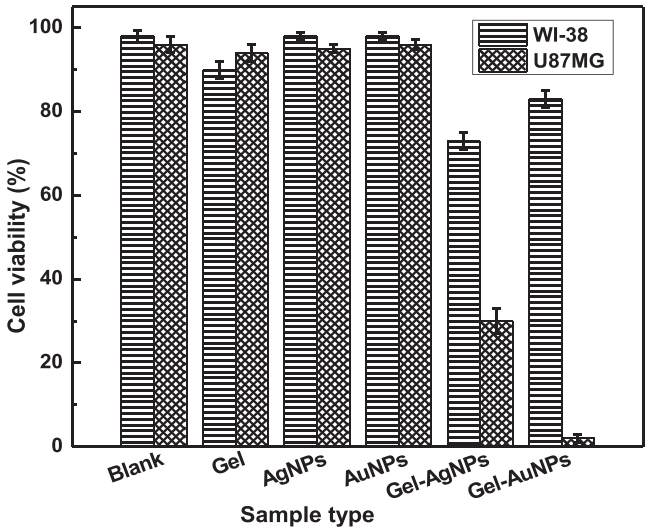

FIGURE 10 Cell viability (%) of normal (WI-38) and cancer (U87MG) cell lines cultured in solution (NPs) and on the surface of different samples for 48 hours

and their HNCs are shown here. This cytocompatibility of our pure NPs (Ag and AuNPs) with the optimum size used here (30 to 50 nm) was in in good agreement with a previous report, where the size dependent cytotoxicity was investigated by in vitro and in vivo models. AuNPs in the range of 20 to 50 nm was non-cytotoxic as no indication of DNA damage was observed, while smaller NPs of size 4–5 nm caused significant DNA damage. [40] The percentage cell viability (%) on the surface of different gel compositions was calculated according to a previous protocol.[41]

The anticancer efficacy of the designed HNCs (Figure 9) was investigated by an in vitro assay against cancer cells (primary glioblastoma cell lines) (U87MG) for 48 hours using blank cell culture media as a control. The HNCs of AgNPs were less effective against these cells (E) than AuNPs-incorporated HNCs (D). Comparing the cell viability (%) data (Figure 10) of the two kinds of cells (WI-38 and U87MG) further explains that HNCs of AgNPs (gel-AgNPs) have comparatively lower cell viability (75 ± 2%) against normal cells (WI-38) and have higher cell viability (30 ± 3%) against cancer cells (U87MG). On the other hand the HNCs of AuNPs (gel-AuNPs) have good normal cell (WI-38) viability (85 ± 2%) as well as lowest cell viability (2 ± 1%) against cancer (U87MG) cells. This indicates that the HNCs of AuNPs (gel-AuNPs) could be an effective material against cancer cell apoptosis as most of the cells were dead after 48 hours. Note that the overall charge on these AuNPs is negative (Z = -36 mV) and this lowered anticancer effect on U87MG cells of pure AgNPs is due to electrostatic repulsion with the negatively charged cell membrane (lower cellular uptake). Therefore, in the case of HNCs, it is possible that the cationic hydrogel chain would screen repulsive forces by covering NPs surface and hence provides EPR effect.[42]

It is also reported that the cellular uptake depends on particle surface functionalization, and the positively charged NPs have higher cellular uptake than neutral and negatively charged, which after injection into cytoplasm via endocytosis enters into the nucleus or permeabilize the mitochondrial membrane to release apoptogenic factors like cytochrome c, which activate caspasis and cellular death.[43,44] Therefore, these hybrid hydrogels with incorporated gold nanoparticles (HNCs-AuNPs) are serving by active targeting mechanism to completely kill cells and stop cancer cell growth.

4 | CONCLUSIONS

The biobased self-healing composite hydrogel was obtained from renewable biopolymer, chitosan- and aldehyde-terminated star-branched PEG crosslinker by dynamic Schiff-base crosslinking reaction. The gel components were investigated by physicochemical characterization techniques confirming the successful

functionalization. The mechanical characterization of the hydrogels was investigated as a function of polymer/crosslinker ratios and total solid content (T%), which indicated that their moduli were dependent on both these parameters. The gel was self-healable/injectable at an appropriate polymer/crosslinker ratio of 1:1 and total solid content (T = 2%). The hydrogel nanocomposites (HNCs) with AgNPs and AuNPs were investigated for biocompatibility against WI-38 cells for 48 hours, which showed good biocompatibility. The HNCs were tested for anticancer activity against U87 MG for 48 hours, which indicated that as against pure gels and pure MNPs, the HNCs decorated with AuNPs were effective against cancer cell apoptosis. Therefore, the chitosan-PEG/AuNPs hydrogel nanocomposites could be an effective material for the future anticancer nanomedicine.

ACKNOWLEDGEMENTS

The authors acknowledge Tampere University of Technology (internal funding for postdoctoral researchers) and Business Finland (former TEKES - Finnish Funding Agency for Innovation) project Human Spare Parts for financially supporting this work.

CONFLICTS OF INTEREST

There are no conflicts of interest to declare for this study.

REFERENCES

1. A. E. Forte, S. Galvan, F. Manieri, F. R. Baena, D. Dini, *Mater. Des.* **2016**, *112*, 227. https://www.sciencedirect.com/science/article/pii/S0264127516312370?via%3Dihub.
2. M. Biondi, A. Borzacchiello, L. Mayol, L. Ambrosio, *Gels*, **2015**, *1*, 162.
3. N. I. M. Fadilah, I. L. M. Isa, W. S. W. K. Zaman, Y. Tabata, M. B. Fauzi, *Polymers* **2022**, *14*, 476.
4. D. Liang, Z. Lu, H. Yang, J. Gao, R. Chen, *ACS Appl. Mater. Interfaces* **2016**, *8*(6), 3958.
5. H. Sashiwa, S. Aiba, *Prog. Polym. Sci.* **2004**, *29*, 887.
6. N. Bhattarai, H. R. Ramay, J. Gunn, F. A. Matsenb, M. Zhang, *J. Control. Release*, **2005**, *103*, 609.
7. F. R. De Abreu, S. P. Campana-Filho, *Carbohydr. Polym.* **2009**, *75*(2), 214. https://linkinghub.elsevier.com/retrieve/pii/S0144861708002890.
8. B. Xiao, Y. Wan, M. Zhao, Y. Liu, S. Zhang, *Carbohydr. Polym.* **2011**, *83*(1), 144. https://www.sciencedirect.com/science/article/abs/pii/S0144861710005758?via%3Dihub.
9. S. Fattahpour, M. Shamanian, N. Tavakoli, M. Fathi, H. Sadeghi-aliabadi, S. R. Sheykhi, M. Fesharaki, S. Fattahpour, *Int. J. Biol. Macromol.* **2020**, *151*, 220.
10. K. Kim, J. H. Ryu, D. Y. Lee, H. Lee, *Biomater. Sci.* **2013**, *1*, 783.
11. Q. Hu, T. Wang, M. Zhou, J. Xue, Y. Luo, *J. Agric. Food Chem.* **2016**, *64*, 5893.
12. L. Cao, B. Cao, C. Lu, G. Wang, L. Yu, J. Ding, *J. Mater. Chem. B* **2015**, *3*, 1268.
13. M. Khan, S. Schuster, M. Zharnikov, *Phys. Chem. Chem. Phys.* **2016**, *18*, 12035.
14. M. T. Mansouri, Y. Farbood, M. J. Sameri, A. Sarkaki, B. Naghizadeh, M. Rafeirad, *Food Chem*. **2013**, *138*, 1028.
15. G. V. Haute, E. Caberlon, E. Squizani, F. C. de Mesquita, L. Pedrazza, B. A. Martha, et al. *Toxicol. In Vitro*, **2015**, *30*, 309.
16. M. Xie, B. Hu, Y. Wang, X. Zeng, *J. Agric. Food Chem.* **2014**, *62*, 9128.
17. O. Ramirez, S. Bonardd, C. Saldías, D. Radic, A. Leiva, *ACS Appl. Mater. Interfaces* **2017**, *9*(19), 16561.
18. M. Khan, F. Ahmad, J. T. Koivisto, M. Kellomäki, *Colloids Interface Sci. Commun.* **2020**, *39*, 100322. https://www.sciencedirect.com/science/article/abs/pii/S2215038220301023.
19. C. D. Carlo, A. Curulli, R. G. Toro, C. Bianchini, T. De Caro, G. Padeletti, D. Zane, G. M. Ingo, *Langmuir* **2012**, *28*, 5471.
20. S. Bhattacharya, S. K. Samanta, *Chem. Rev.* **2016**, *116*, 11967.
21. W. Huang, Y. Wang, Y. Chen, Y. Zhao, Q. Zhang, X. Zheng, L. Chen, L. Zhang, *Adv. Healthcare Mater.* **2016**, *5*, 2813.
22. D. L. Taylor, M. H. Panhuis, *Adv. Mater.* **2016**, *28*, 9060.
23. P. K. Jain, I. H. El-Sayed Mostafa, A. El-Sayed, *Nanotoday* **2007**, *2*(1), 18.
24. W. Li, Z. Cao, R. Liu, L. Liu, H. Li, X. Li, Y. Chen, C. Lu, Y. Liu, *Artif. Cells Nanomed. Biotechnol.* **2019**, *47*, 4222.
25. Y. Herdiana, N. Wathoni, S. Shamsuddin, M. Joni, M. Muchtaridi, *Polymers* **2021**, *13*, 1717.
26. N. Moramkar, P. Bhatt, *Eur. Polym. J.* **2021**, *154*, 110540. https://www.sciencedirect.com/science/article/abs/pii/S0014305721002743.
27. M. S. Shakil, K. M. Mahmud, M. Sayem, M. S. Niloy, S. K. Halder, M. S. Hossen, M. F. Uddin, M. A. Hasan, *Polysaccharides* **2021**, *2*(4), 795. https://www.mdpi.com/2673-4176/2/4/48.
28. J. Shang, X. Gao, *Chem. Soc. Rev.* **2014**, *43*(21), 7267.
29. M. Khan, J. T. Koivisto, T. I. Hukka, M. Hukka, M. Kellomaki, *ACS Appl. Mater. Interfaces* **2018**, *10*, 11950.
30. Y. Zeng, X. Wang, J. Wang, R. Yi, H. Long, M. Zhou, Q. Luo, Z. Zhai, Y. Song, S. Qi, *Cell Mol. Neurobiol.* **2018**, *38*(6), 1245.
31. S. Zheng, X. Li, Y. Zhang, Q. Xie, Y.S. Wong, W. Zheng, T. Chen, *Internat. J. Nanomed.* **2012**, *7*, 3939.
32. R. Mathiyalagan, Y. J. Kim, C. Wang, Y. S. Jinb, P. S. Subramaniyam, D. Wang, D. C. Yang, *Artificial Cells Nanomed. Biotechnol.* **2016**, *44*(8), 1803. https://pubmed.ncbi.nlm.nih.gov/26539976/.
33. J. M. Lee, J. H. Kim, K. W. Kim, B. J. Lee, D. G. Kim, Y.O. Kim, J. H. Lee, I. S. Kong, *Int. J. Biol. Macromol.* **2018**, *108*, 598.
34. J. Kumirska, M. Czerwicka, Z. Kaczyński, A. Bychowska, K. Brzozowski, J. Thöming, P. Stepnowski, *Mar. Drugs* **2010**, *8*, 1567.
35. V. Dmitrovic, G. J. M. Habraken, M. M. R. M Hendrix, W. J. E. M. Habraken, A. Heise, G. de With, N. A. J. M. Sommerdijk, *Polymers* **2012**, *4*(2), 1195. https://www.mdpi.com/2073-4360/4/2/1195.
36. D. Arizmendi-Cotero, R. M. Gómez-Espinosa, O. D. García, V. Gómez-Vidales, A. Dominguez-Lopez, *Carbohydr. Polym.* **2016**, *136*, 350.
37. M. Catauro, S. V. Ciprioti, *Crit. Rev.* **2021**, *14*(7), 1788.
38. T. Groth P. Falck, R. G. Miethke, *ATLA*. **1995**, *23*, 790.
39. E. Jablonská, J. Kubásek, D. Vojtěch, T. Ruml, J. Lipov, *Sci Rep.* **2021**, *11*, 6628.
40. Q. Xia, S. Zhang, Q. Feng, K. Xiao, H. Li, Y. Liu, *J. Biomed. Mater. Res. Part A* **2017**, *105*(3), 710. https://onlinelibrary.wiley.com/doi/10.1002/jbm.a.35944.

41. N. K Sahu, N. S. Singh, L. Pradhan, D. Bahadur, *Dalton Trans.* **2014**, *43*, 11728.
42. E. C. Dreaden, L. A. Austin, M. A. Mackey, M. A. El-Sayed, *Thera. Deliv.* **2012**, *3*(4), 457.
43. S. Siddique. J. C. L. Chow, *Appl. Sci.* **2020**, *10*(11), 3824. https://www.mdpi.com/2076-3417/10/11/3824.
44. A. P. Daduang, S. Daduang, P. Suwannalert, T. Limpaiboon, *Asian Pac. J. Cancer Prev.* **2015**, *16*(1), 169.

How to cite this article: M. Khan, J. T. Koivisto, M. Kellomäki. *Nano Select*. **2022**, *3,* 1213.
https://doi.org/10.1002/nano.202100354